

# Witnessing Short- and Long-Range Nonstabilizerness via the Information Lattice

Yuliya Bilinskaya,<sup>\*</sup> Miguel F. Martínez,<sup>\*</sup> Soumi Ghosh,

Thomas Klein Kvorning, Claudia Artiano, and Jens H. Bardarson

*Department of Physics, KTH Royal Institute of Technology, 106 91, Stockholm, Sweden*

We study nonstabilizerness on the information lattice, and demonstrate that noninteger local information directly indicates nonstabilizerness. For states with a clear separation of short- and large-scale information, noninteger total information at large scales  $\Gamma$  serves as a witness of long-range nonstabilizerness. We propose a folding procedure to separate the global and edge-to-edge contributions to  $\Gamma$ . As an example we show that the ferromagnetic ground state of the spin-1/2 three-state Potts model has long-range nonstabilizerness originating from global correlations, while the paramagnetic ground state has at most short-range nonstabilizerness.

*Introduction*—Quantum information theory offers a unifying lens for understanding quantum states and dynamics [1–9]. In the context of condensed matter, states are often classified in terms of the scaling of the subsystem von Neumann entropy, which is a global measure of the total correlations between a subsystem and its complement. In area-law states [1–4], such as ground states of local gapped Hamiltonians and many-body localized states, correlations are mainly local, meaning that the von Neumann entropy of a subsystem scales with its area. This enables efficient representation of such states via matrix product states [4, 10, 11]. In contrast, volume-law states [5–7], such as mid-spectrum eigenstates of ergodic Hamiltonians, have correlations involving an extensive number of degrees of freedom. Furthermore, constant subleading corrections to the area-law scaling serve to characterize states with topological order [12–16].

Quantum states can also be characterized by other quantum information properties such as nonstabilizerness. Stabilizer states are the class of states that are closed under Clifford operations and they admit an efficient classical representation by the Gottesman-Knill theorem [17, 18]. Generic condensed matter states fall outside this class as they require non-Clifford unitaries to be reached from a stabilizer state. Such unitaries are constructed from the elements of a universal set realized, for example, by the combination of Clifford and  $T$ -gates. The deviation of a state from a stabilizer state is known as nonstabilizerness, or magic, and has been quantified in the literature by different measures [19–27]. While the concept of nonstabilizerness arose in the context of quantum error correction and fault tolerant quantum computation [28–31], they have increasing relevance in condensed matter and quantum many-body physics [32–47].

Nonstabilizerness has been interpreted as a measure of quantum-state complexity [38, 46, 48–51] as it quantifies the distance from the easily representable stabilizer states. Other measures based on the distance from other classes of states that admit efficient representations, such as area-law or fermionic Gaussian states [50, 52, 53], provide similar yet inequivalent quantifications of complexity. The existence of different classes of states that admit effi-

cient representations raises the requirement of a broader classification. For instance, a comprehensive characterization of quantum states can be obtained by looking at the scale of both correlations and nonstabilizerness.

From the point of view of correlations, the information lattice [54, 55] provides a universal characterization of quantum states in terms of local information, which quantifies the total amount of correlations per scale  $\ell$  and spatial location  $n$ . The information lattice defines the intrinsic correlation length scales of a state, which do not depend on any specific observable [55]. Within the information lattice, local information behaves as a hydrodynamic quantity: under the application of a local quantum gate, information can only flow between nearby lattice points and there exist well-defined information currents [54]. This allows to comprehensively characterize quantum quench dynamics [56, 57] and to perform efficient time evolution of large-scale quantum many-body systems [54, 58, 59]. As opposed to information, there is no well-defined decomposition indicating where and on what scale nonstabilizerness resides, but there are attempts to evaluate nonlocality of nonstabilizerness [60–65], as well as to divide nonstabilizerness into short- and long-range [66–68]. The latter approach relies on an equivalence relation up to shallow local unitary quantum circuits as is done in topological classification [15].

In this work we show that any noninteger value of local information on the information lattice directly indicates nonstabilizerness in a quantum state. Furthermore, in states where there is a clear separation between short- and large-scale local information (we refer to such states as localized), we use the information lattice to define a witness of long-range nonstabilizerness via the total information at large scales  $\Gamma$  [55]. Through a folding procedure, we define a coarse-grained information lattice that allows us to distinguish whether the long-range nonstabilizerness originates from global or edge-to-edge correlations. We exemplify our approach using the spin-1/2 three-state Potts model and characterize its ground states in the paramagnetic and ferromagnetic phases in terms of their nonstabilizerness. While the paramagnetic ground state has at most short-range nonstabilizerness, the ferromag-

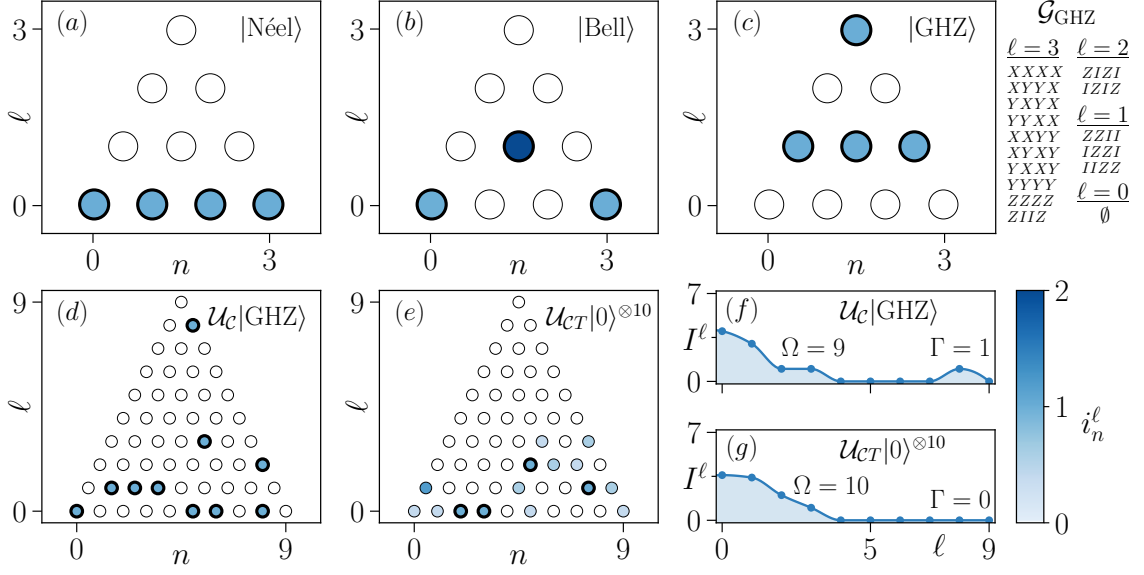


FIG. 1. Information lattice of (a)  $|\text{Néel}\rangle = |0101\rangle$ , (b)  $|\text{Bell}\rangle = \frac{1}{\sqrt{2}}(|0101\rangle + |0011\rangle)$ , and (c)  $|\text{GHZ}\rangle = \frac{1}{\sqrt{2}}(|0000\rangle + |1111\rangle)$ . The right side shows the stabilizer group  $\mathcal{G}_{\text{GHZ}}$  of the four-qubit GHZ state (excluding the identity operator). (d) Information lattice of a stabilizer state constructed by applying a 2-layer random Clifford circuit  $\mathcal{U}_C$  to the ten-qubit GHZ state. (e) Information lattice of a short-range nonstabilizer state constructed by applying a random  $T$ -doped Clifford circuit  $\mathcal{U}_{CT}$  on the product state  $|0\rangle^{\otimes 10}$ . The circuit  $\mathcal{U}_{CT}$  is composed of three blocks, each one containing 10 layers of Clifford gates and 5  $T$ -gates acting on randomly-selected qubits and between two randomly selected Clifford layers. (f, g) Information per scale  $I^\ell$  of (d) and (e) respectively. In (a-e) the sites of the information lattice with integer values of local information are highlighted with a bold black line encircling the site.

netic ground state exhibits long-range nonstabilizerness originating from global correlations.

*Stabilizer states and the information lattice*—We consider an  $L$ -qubit chain with Hilbert space  $\mathcal{H} = (\mathbb{C}^2)^{\otimes L}$ . We denote by  $\mathcal{C}_n^\ell$  the subsystem of  $\ell + 1$  contiguous sites centered at position  $n$ , and refer to  $\ell$  as the scale of  $\mathcal{C}_n^\ell$ . The information lattice of a state  $\rho$  acting on  $\mathcal{H}$  is a two-dimensional structure where subsystems are ordered hierarchically in terms of location  $n$  and scale  $\ell$  [54, 55]. Each site in this structure is uniquely specified by the pair  $(n, \ell)$  and is associated with local information  $i_n^\ell$  in subsystem  $\mathcal{C}_n^\ell$ . The local information is the maximal amount of information one can obtain by measuring any set of operators that cannot be accessed from any smaller-scale subsystem of  $\mathcal{C}_n^\ell$  [54, 55]. The local information is strictly positive and bounded by two from above,  $i_n^\ell \in [0, 2]$ . The information lattice thereby provides a decomposition of the total information  $I(\rho) = \sum_{(n, \ell)} i_n^\ell$  into local information  $i_n^\ell$ .

Stabilizer states are characterized by featuring only integer values of local information, owing to their particular entanglement structure [69, 70]. A stabilizer state is the simultaneous  $+1$  eigenvector of  $2^L$  Pauli strings, which together form an abelian group called the stabilizer group.

Every stabilizer group is generated by  $L$  independent Pauli strings. For a stabilizer state, the operators that yield a maximal amount of information in every subsystem are given by a particular set of stabilizer generators that we call the maximally local generating set [70]. The elements of this set are found at each scale, starting from  $\ell = 0$ , by selecting the maximum number of independent Pauli strings on that scale belonging to the stabilizer group. This construction continues until there are  $L$  independent Pauli strings in the set. The measurement of each of these operators answers a binary question corresponding to one bit of information—namely, whether or not the state is stabilized by the operator—which results in an integer local information for every subsystem.

In Fig. 1(a) we show the information lattice of the four-qubit Néel state  $|\text{Néel}\rangle = |0101\rangle$  as an example. The maximally local generating set for this state is given by  $\{ZIII, -IZII, IIZI, -IIIZ\}$ . In this case, the measurement of each of these operators answers whether the qubit where the operator acts nontrivially is in state  $|0\rangle$  or  $|1\rangle$ . The information gained by each of these binary questions is associated with the corresponding site on the information lattice, yielding a local information  $i_n^\ell = \delta_{\ell,0}$  fully contained at scale  $\ell = 0$ .

As a second example consider the state  $|\text{Bell}\rangle = \frac{1}{\sqrt{2}}(|0101\rangle + |0011\rangle)$  in which the two center qubits are maximally entangled with each other. The information lattice of this state is shown in Fig. 1(b). The two edge qubits are the same as in the previous example, which means that the operators  $ZIII$  and  $-IIIZ$  still belong to the maximally local generating set and correspond to the local information  $i_0^0 = i_3^0 = 1$ . The two bits of information associated with the maximally entangled pair at the center are only accessible by measuring two-qubit operators. This is reflected in the information lattice of the state, where  $i_1^0 = i_2^0 = 0$  and  $i_{1.5}^1 = 2$ . There are three possible operators that fulfill this constraint:  $IXXI$ ,  $IYYI$ , and  $IZZ I$ . As all three are not independent, it is enough to pick any two of them to complete the maximally local generating set.

As a final example, consider the 4-qubit GHZ state,  $|\text{GHZ}\rangle = \frac{1}{\sqrt{2}}(|0000\rangle + |1111\rangle)$ , whose information lattice and stabilizer group are given in Fig. 1(c). The local information of the subsystems at scale  $\ell = 1$  is  $i_n^1 = 1$  and is associated with the measurement of the stabilizer operators at that scale:  $ZZII$ ,  $IZZ I$ , and  $IIZZ$ . These operators are independent of each other and belong to the maximally local generating set. At scale  $\ell = 2$  there are no stabilizer operators independent from the ones at  $\ell = 1$ , yielding  $i_1^2 = i_3^2 = 0$ . The remaining bit of information  $i_{1.5}^3 = 1$  is located at the largest scale and can only be accessed by measuring an operator that has nontrivial support on the scale of the entire system. There are ten possible stabilizer operators at the largest scale, and only eight are independent from the stabilizer operators at  $\ell = 1$ . Choosing one of them, for example  $XXXX$ , completes a maximally local generating set for the GHZ state. In general, as demonstrated in this and the second examples, the maximally local generating set may not be unique. However, the locality of its operators, dictated by the position of the nonzero local information on the information lattice, is.

Formally, the local information  $i_n^\ell$  is

$$i_n^\ell = I(\rho_n^\ell) - I(\rho_{n-1/2}^{\ell-1}) - I(\rho_{n+1/2}^{\ell-1}) + I(\rho_n^{\ell-2}), \quad (1)$$

where  $I(\rho_n^\ell) = (\ell+1) - S(\rho_n^\ell)$  is the total information with  $S(\rho_n^\ell) = -\text{Tr}[\rho_n^\ell \log_2(\rho_n^\ell)]$  the von Neumann entropy of subsystem  $\mathcal{C}_n^\ell$ . For a stabilizer state,  $I(\rho_n^\ell) = |\mathcal{G}_n^\ell| \leq \ell+1$ , where  $|\cdot|$  denotes the rank of a group [69], defined as the number of elements in its generating set (see appendix for details).  $\mathcal{G}_n^\ell$  is the stabilizer subgroup of subsystem  $\mathcal{C}_n^\ell$ , which contains the elements of the stabilizer group with trivial support in the complement of  $\mathcal{C}_n^\ell$ . Consequently, the local information becomes

$$i_n^\ell = |\mathcal{G}_n^\ell| - |\mathcal{G}_{n-1/2}^{\ell-1}| - |\mathcal{G}_{n+1/2}^{\ell-1}| + |\mathcal{G}_n^{\ell-2}|, \quad (2)$$

which is integer-valued and corresponds to the number of independent generators acting nontrivially only at scale

$\ell$ . This is consistent with the fact that local information is bounded by two from above: increasing a subsystem by one site adds at most two additional independent generators to the maximally local generating set.

*Short- and long-range nonstabilizerness via the information lattice*—A quantum state has nonstabilizerness if it is not a stabilizer state. Since a stabilizer state necessarily has  $i_n^\ell \in \mathbb{N}$ , a state with any noninteger value of  $i_n^\ell$  has nonstabilizerness. This is exemplified in Fig. 1(d,e), where we show the information lattice of a stabilizer state constructed by applying a random Clifford circuit to the ten-qubit GHZ state, and that of a nonstabilizer state constructed by applying a  $T$ -doped Clifford circuit to the product state  $|0\rangle^{\otimes 10}$ .

We classify nonstabilizerness in terms of its locality by distinguishing short- and long-range nonstabilizer states [66–68]. A state has short-range nonstabilizerness if it can be transformed into a stabilizer state by a shallow local unitary circuit, while a long-range nonstabilizer state requires a local unitary circuit that scales with the system size. To capture these two classes of nonstabilizerness we use the information lattice, which has been shown to classify quantum states in terms of the information per scale,

$$I^\ell = \sum_n i_n^\ell. \quad (3)$$

We are interested in localized states, which exhibit an extensive amount of information per scale at  $\ell \ll L$ , captured by

$$\Omega = \sum_{\ell=0}^{\lfloor L/2-1 \rfloor} i_n^\ell. \quad (4)$$

Examples of such states are the ground states of local Hamiltonians and eigenstates of many-body localized systems. Some localized states may also have an intensive  $\mathcal{O}(1)$  contribution to local information at scales  $\ell \sim L$ . This contribution may originate from edge-to-edge correlations, as for example in symmetry-protected topological states, or global correlations, as in cat states [55]. In localized states, the information per scale  $I^\ell$  decays exponentially away from the information peaks both at short and large scales, creating an information gap, see Fig. 1(f, g). While the information gap is extensive, the  $\mathcal{O}(1)$  contribution at large scales stays constant and is captured by the total information at large scales

$$\Gamma = \sum_{\ell=\lfloor L/2 \rfloor}^{L-1} i_n^\ell, \quad (5)$$

which serves as a universal characteristic of topological phases [55]. In Fig. 1(f, g) we show the total information per scale of states in Fig. 1(d, e) and calculate the corresponding values of  $\Gamma$  and  $\Omega$ .

Under a local unitary circuit the information flow on the information lattice is strictly local. As a result the only way to close the information gap and redistribute information between  $\Omega$  and  $\Gamma$  is by applying a circuit that scales with the system size. Consequently, a localized state with noninteger  $\Gamma$  cannot be transformed into a stabilizer state, which always has integer  $\Gamma$ , by any shallow local unitary circuit. Thus,  $\Gamma \notin \mathbb{N}$  is a witness of long-range nonstabilizerness for localized states. This implies that a localized state with  $\Gamma = 0$  can have at most short-range nonstabilizerness, as for example is the case for the state in Fig. 1(e).

In localized states in the thermodynamic limit, the total information at large scales  $\Gamma$  separates into contributions coming from edge-to-edge and global correlations, such that  $\Gamma =: \gamma_{\text{edge}} + \gamma_{\text{global}}$ . To estimate  $\gamma_{\text{global}}$  in a given state, we employ a folding procedure in which sites  $n$  and  $L - n - 1$  are combined, reducing the chain length by half, while doubling the local Hilbert space dimension at each site. Due to this coarse graining the edge-to-edge correlations of the initial chain become local on the information lattice of the folded chain. Therefore, only the global correlations survive at large scales and the total information at large scales of the folded information lattice  $\Gamma_{\text{folded}}$  provides an estimate of  $\gamma_{\text{global}}$ . The folding procedure is exemplified in Fig. 2(a).

Long-range nonstabilizerness may arise in quantum systems when the ground state of the Hamiltonian is degenerate. This occurs, for example, when there is a spontaneously broken symmetry. In the symmetric ground state,  $\log_2(q)$  bits of information are associated with the relative phases between the different  $q$  degenerate states breaking the symmetry. This results in  $\Gamma = \log_2(q)$ , thus  $q \neq 2^x$  with  $x \in \mathbb{N}$  implies  $\Gamma \notin \mathbb{N}$  and long-range nonstabilizerness. In the next section, we show that these conditions are realized in the ground state of the spin-1/2 three-state Potts model.

*Spin-1/2 three-state Potts model*—The three-state Potts model [71] is described by the Hamiltonian

$$H = -\frac{J}{3} \sum_i^{N-1} (Z_i^\dagger Z_{i+1} + Z_i Z_{i+1}^\dagger) - h \sum_i^N (X_i^\dagger + X_i), \quad (6)$$

$$Z_i = \begin{pmatrix} 1 & 0 & 0 \\ 0 & \omega & 0 \\ 0 & 0 & \omega^2 \end{pmatrix}, \quad X_i = \begin{pmatrix} 0 & 0 & 1 \\ 1 & 0 & 0 \\ 0 & 1 & 0 \end{pmatrix}, \quad (7)$$

with  $J, h \geq 0$  the interaction strength and the transverse magnetic field respectively, and  $\omega = e^{2\pi i/3}$ . This model has a  $\mathbb{Z}_3$  rotational symmetry realized by  $\prod_{i=1}^N X_i$ , and undergoes a phase transition at the self-dual point  $J/3 = h$  between a symmetry-broken phase with a three-fold degenerate ground state and a paramagnetic phase with a unique ground state [72]. We realize this model in a spin-1/2 chain of length  $L = 2N$  by projecting each pair of neighboring spins onto the triplet subspace, onto which the operators  $Z_i$  and  $X_i$  act.

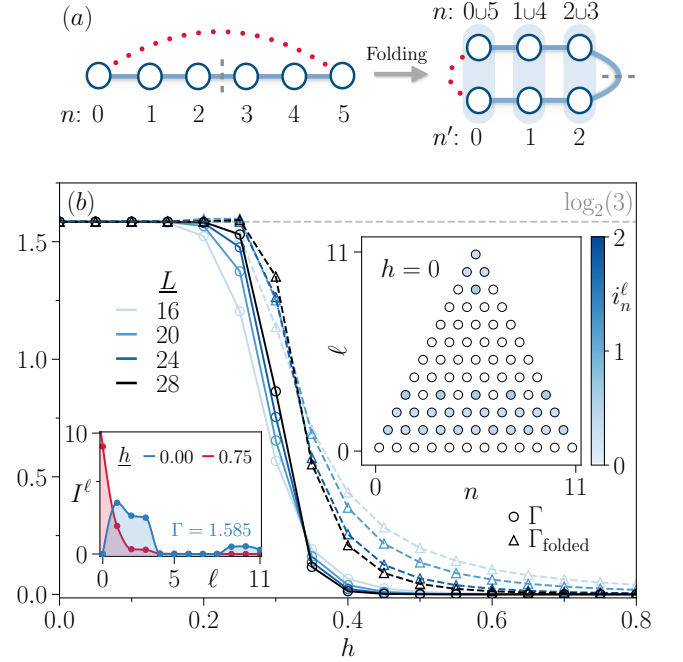


FIG. 2. (a) Sketch of the folding procedure used to estimate  $\gamma_{\text{global}}$  in a chain of length  $L = 6$ . The chain is folded across the gray dashed line at its middle point, resulting in a folded chain of length  $L' = 3$ . The sites in the folded chain are given by the blue ovals, denoted by  $n'$ , and encompass those sites of the unfolded chain,  $n$ , belonging to each oval. The dotted red line sketches an edge-to-edge correlation between sites  $n = 0$  and  $n = 5$  in the unfolded chain, which becomes completely local to site  $n' = 0$  in the folded chain. (b) The total information at large scales in the unfolded and folded chain of the symmetric ground state of the spin-1/2 three-state Potts model, as a function of the magnetic field  $h$  and system size  $L$ , with  $J = 1$ . The right inset depicts the information lattice of the symmetric ground state at  $h = 0$  and  $L = 12$ . The left inset shows the information per scale for the same state (blue line) and for the paramagnetic ground state at  $h = 0.75$  and  $L = 12$ .

We characterize the nonstabilizerness in the symmetric ground state for different values of  $h$  and  $L$  at fixed  $J = 1$ . The information lattice of the symmetric ground state for a small magnetic field  $h \ll 1/3$  is shown in the right inset of Fig. 2(b) with  $h = 0$  and  $L = 12$ . There is an extensive amount of information at small scales  $\Omega \sim \mathcal{O}(L)$  and a finite contribution at large scales  $\Gamma$  separated by an information gap. The same features are also clearly visible in the information per scale as shown in the left inset (blue line) of Fig. 2(b). The noninteger  $\Gamma \approx \log_2(3)$  in the presence of an information gap indicates the long-range nonstabilizerness of the state. For  $h \gg 1/3$  the value of  $\Gamma$  goes to zero (red line in the left inset), and local information is present at small scales only, which indicates at most short-range nonstabilizerness. In the main panel of Fig. 2(b) we show both  $\Gamma$  and  $\Gamma_{\text{folded}}$  as functions of  $h$  for different system sizes  $L$ , where curves for different  $L$



cross approximately at the phase transition point  $h = 1/3$ . There is a systematic flow on both sides of the crossings such that  $\Gamma$  and  $\Gamma_{\text{folded}}$  approach either  $\log_2(3)$  or 0 as  $L$  increases. Away from the critical point, for  $h \lesssim 0.2$ , the total information at large scales for the folded information lattice is  $\Gamma_{\text{folded}} \approx \Gamma$ , which indicates that long-range nonstabilizerness originates from global correlations. In the vicinity of the critical point the information gap closes and there is nonzero local information at all scales. Thus  $\Gamma$  scales with system size and is no longer a witness of long-range nonstabilizerness. In this case, the folding procedure rearranges local information on the folded information lattice such that there are additional contributions at large scales making  $\Gamma_{\text{folded}}$  overestimate the global correlations  $\gamma_{\text{global}}$ .

*Discussion*—We have shown that the information lattice provides a straightforward and direct way to identify nonstabilizerness in any quantum state. This stems from the fact that local information in a stabilizer state is necessarily an integer. In localized states, defined by the presence of an information gap, the information lattice allows to detect long-range nonstabilizerness. The information gap prevents the redistribution of information between short and large scales under shallow local unitary circuits making the total information at large scales  $\Gamma$  an invariant. As a consequence, a noninteger  $\Gamma$  serves as a witness of long-range nonstabilizerness, since it indicates that a state cannot be transformed into a stabilizer state by any shallow local unitary circuit. Using a folding procedure we further identify global and edge-to-edge contributions to  $\Gamma$ . Our method directly witnesses long-range nonstabilizerness without the need of employing any minimization procedure or a search for a shallow local unitary circuit connecting the state to a stabilizer state.

As an example we have analyzed the long-range nonstabilizerness of the spin-1/2 three-state Potts model. At small magnetic field the symmetric ground state of the model has large-scale information  $\Gamma \approx \log_2(3)$ , indicating long-range nonstabilizerness. This comes directly from the fact that the ground state is threefold degenerate. For a large magnetic field  $\Gamma \approx 0$  indicates at most short-range nonstabilizerness. At the phase transition between these two limits the ground state is no longer localized as the information gap closes and  $\Gamma$  cannot be used as a witness of long-range nonstabilizerness.

Since the information lattice is a state property, our approach is independent of any parent Hamiltonian or any protocol used to generate quantum states and aids in the current efforts to characterize states in terms of the scale of their nonstabilizerness. Our results extend to states with multiple information gaps, where the total information at large scales  $\Gamma$  is redefined as the sum of local information from scale  $\ell = L - 1$  down to the largest  $\ell$  where an information gap resides. The properties discussed in this paper are also potentially accessible through experiments as the density matrix can be reconstructed experimentally

through quantum state tomography [73–77].

While in this work we focused on one-dimensional systems, a possible future direction is to study nonstabilizerness in localized states in higher dimensions. Our framework can be readily used via a quasi-1d approach, in which the information lattice of an effective one-dimensional system is obtained by coarse-graining a higher-dimensional system. More generally, one could explore long-range nonstabilizerness in higher dimensions via a higher-dimensional local decomposition of information [78]. Another direction is to explore nonstabilizerness in mixed-state phases [79, 80], to which the information lattice is directly applicable. Furthermore, generalizing the characterization of quantum states by the scale of their nonstabilizerness requires constructing a fully local decomposition of nonstabilizerness akin to the information lattice. This is, for example, relevant for characterizing critical and ergodic states.

*Acknowledgments*—We thank D. Aceituno Chávez, I. M. Flór and A. Partos for useful discussions. This work received funding from the European Research Council (ERC) under the European Union’s Horizon 2020 research and innovation program (Grant Agreement No. 101001902) and the Knut and Alice Wallenberg Foundation (KAW) via the project Dynamic Quantum Matter (2019.0068). T. K. K. acknowledges funding from the Wenner-Gren Foundations. The computations were enabled by resources provided by the National Academic Infrastructure for Supercomputing in Sweden (NAISS), partially funded by the Swedish Research Council through grant agreement no. 2022-06725.

## Appendix: von Neumann entropy in a stabilizer state

Following Ref. 69, the density matrix of an  $L$ -qubit stabilizer state  $|\psi\rangle = \mathcal{U}_C |0\rangle^{\otimes L}$ , where  $\mathcal{U}_C$  is a Clifford circuit, can be written in the form

$$\rho = |\psi\rangle\langle\psi| = \mathcal{U}_C |0\rangle^{\otimes L} \langle 0|^{\otimes L} \mathcal{U}_C^\dagger = \mathcal{U}_C \prod_i^L \frac{\mathbb{I} + Z_i}{2} \mathcal{U}_C^\dagger = \frac{1}{2^L} \prod_i^L (\mathbb{I} + g_i) = \frac{1}{2^L} \sum_{g \in \mathcal{G}} g, \quad (8)$$

where  $\mathbb{I}$  is the identity matrix,  $g$  are the elements of the stabilizer group  $\mathcal{G}$  of the state and  $g_i$  are the generators. Decomposing the chain into two disjoint subsystems,  $A$  and  $B$ , the reduced density matrix of subsystem  $A$  can be written as

$$\rho_A = \text{Tr}_B(\rho) = \text{Tr}_B \left( \frac{1}{2^L} \sum_{g \in \mathcal{G}} g \right) = \frac{1}{2^L} \sum_{g \in \mathcal{G}} \text{Tr}(g_B) g_A = \frac{2^{L_B}}{2^L} \sum_{g_A \in \mathcal{G}_A} g_A = \frac{1}{2^{L_A}} \sum_{g_A \in \mathcal{G}_A} g_A, \quad (9)$$

where  $\mathcal{G}_A$  is the stabilizer subgroup for subsystem  $A$ ,  $L = L_A + L_B$  and we used that the trace of any Pauli matrix vanishes except in the case of identity, which gives  $2^N$ . The von Neumann entropy of subsystem  $A$  can be calculated using that

$$\rho_A^2 = \frac{1}{2^{L_A}} \frac{1}{2^{L_A}} \sum_{g_A \in \mathcal{G}_A} \sum_{\tilde{g}_A \in \mathcal{G}_A} g_A \tilde{g}_A = \frac{1}{2^{L_A}} \sum_{\tilde{g}_A \in \mathcal{G}_A} \left( \frac{1}{2^{L_A}} \sum_{g'_A \in \mathcal{G}_A} g'_A \right) = \frac{\dim(\mathcal{G}_A)}{2^{L_A}} \rho_A. \quad (10)$$

This means that the nonzero eigenvalues of the reduced density matrix of a stabilizer state are completely degenerate and equal to  $\lambda = \dim(\mathcal{G}_A)/2^{L_A}$ , and since  $\rho_A$  has unit trace there are exactly  $2^{N_A}/\dim(\mathcal{G}_A)$  such nonzero eigenvalues. The von Neumann entropy of a subsystem is then given by

$$S(\rho_A) = -\text{Tr}\{\rho_A \log \rho_A\} = -\sum_{\lambda} \lambda \log \lambda = -\frac{2^{L_A}}{\dim(\mathcal{G}_A)} \frac{\dim(\mathcal{G}_A)}{2^{L_A}} \log \left( \frac{\dim(\mathcal{G}_A)}{2^{L_A}} \right) = L_A - |\mathcal{G}_A|, \quad (11)$$

where  $|\mathcal{G}|$  is the rank of the stabilizer subgroup.

---

\* These, alphabetically listed, authors contributed equally to this work.

- [1] M. Srednicki, Entropy and area, *Phys. Rev. Lett.* **71**, 666 (1993).
- [2] M. B. Hastings, An area law for one-dimensional quantum systems, *J. Stat. Mech.* **2007**, P08024 (2007).
- [3] M. M. Wolf, F. Verstraete, M. B. Hastings, and J. I. Cirac, Area laws in quantum systems: Mutual information and correlations, *Phys. Rev. Lett.* **100**, 070502 (2008).
- [4] J. Eisert, M. Cramer, and M. B. Plenio, Colloquium: Area laws for the entanglement entropy, *Rev. Mod. Phys.* **82**, 277 (2010).
- [5] J. M. Deutsch, Quantum statistical mechanics in a closed system, *Phys. Rev. A* **43**, 2046 (1991).
- [6] M. Srednicki, Chaos and quantum thermalization, *Phys. Rev. E* **50**, 888 (1994).
- [7] M. Rigol, V. Dunjko, and M. Olshanii, Thermalization and its mechanism for generic isolated quantum systems, *Nature* **452**, 854 (2008).
- [8] N. Laflorencie, Quantum entanglement in condensed matter systems, *Phys. Rep.* **646**, 1 (2016).
- [9] B. Zeng, X. Chen, D.-L. Zhou, X.-G. Wen, *et al.*, *Quantum information meets quantum matter* (Springer, 2019).
- [10] U. Schollwöck, The density-matrix renormalization group in the age of matrix product states, *Ann. Phys.* **326**, 96 (2011).
- [11] J. I. Cirac, D. Pérez-García, N. Schuch, and F. Verstraete, Matrix product states and projected entangled pair states: Concepts, symmetries, theorems, *Rev. Mod. Phys.* **93**, 045003 (2021).
- [12] A. Hamma, R. Ionicioiu, and P. Zanardi, Ground state entanglement and geometric entropy in the Kitaev model, *Phys. Lett. A* **337**, 22 (2005).
- [13] A. Kitaev and J. Preskill, Topological entanglement entropy, *Phys. Rev. Lett.* **96**, 110404 (2006).
- [14] M. Levin and X.-G. Wen, Detecting topological order in a ground state wave function, *Phys. Rev. Lett.* **96**, 110405 (2006).
- [15] X. Chen, Z.-C. Gu, and X.-G. Wen, Local unitary transformation, long-range quantum entanglement, wave function renormalization, and topological order, *Phys. Rev. B* **82**, 155138 (2010).
- [16] S. Mas-Mendoza, R. D. P. East, M. Filippone, and A. G. Grushin, A graphical diagnostic of topological order using ZX calculus, [arXiv:2509.12355](https://arxiv.org/abs/2509.12355) (2025).
- [17] E. Knill, Non-binary unitary error bases and quantum codes, [arXiv:9608048](https://arxiv.org/abs/9608048) (1996).
- [18] D. Gottesman, The Heisenberg representation of quantum computers, [arXiv:9807006](https://arxiv.org/abs/9807006) (1998).
- [19] J. Emerson, D. Gottesman, S. A. H. Mousavian, and V. Veitch, The resource theory of stabilizer quantum computation, *New J. Phys.* **16**, 013009 (2014).
- [20] M. Howard and E. Campbell, Application of a resource theory for magic states to fault-tolerant quantum computing, *Phys. Rev. Lett.* **118**, 090501 (2017).
- [21] S. Bravyi, D. Browne, P. Calpin, E. Campbell, D. Gosset, and M. Howard, Simulation of quantum circuits by low-rank stabilizer decompositions, *Quantum* **3**, 181 (2019).
- [22] L. Leone, S. F. E. Oliviero, and A. Hamma, Stabilizer Rényi entropy, *Phys. Rev. Lett.* **128**, 050402 (2022).
- [23] J. Jiang and X. Wang, Lower bound for the  $T$  count via unitary stabilizer nullity, *Phys. Rev. Appl.* **19**, 034052 (2023).
- [24] E. Tirrito, P. S. Tarabunga, G. Lami, T. Chanda, L. Leone, S. F. E. Oliviero, M. Dalmonte, M. Collura, and A. Hamma, Quantifying nonstabilizerness through entanglement spectrum flatness, *Phys. Rev. A* **109**, L040401 (2024).
- [25] N. Dowling, P. Kos, and X. Turkeshi, Magic resources of the Heisenberg picture, *Phys. Rev. Lett.* **135**, 050401 (2025).
- [26] N. Dowling, K. Modi, and G. A. L. White, Bridging entanglement and magic resources within operator space, *Phys. Rev. Lett.* **135**, 160201 (2025).
- [27] A. Paviglianiti, G. Lami, M. Collura, and A. Silva, Estimating nonstabilizerness dynamics without simulating it, *PRX Quantum* **6**, 030320 (2025).
- [28] D. Gottesman, Stabilizer codes and quantum error correction, [arXiv:9705052](https://arxiv.org/abs/9705052) (1997).
- [29] D. Gottesman, Theory of fault-tolerant quantum computation, *Phys. Rev. A* **57**, 127 (1998).
- [30] S. Bravyi and A. Kitaev, Universal quantum computation with ideal Clifford gates and noisy ancillas, *Phys. Rev. A* **71**, 022316 (2005).
- [31] A. G. Fowler, M. Mariantoni, J. M. Martinis, and A. N. Cleland, Surface codes: Towards practical large-scale quantum computation, *Phys. Rev. A* **86**, 032324 (2012).
- [32] Z.-W. Liu and A. Winter, Many-body quantum magic, *PRX Quantum* **3**, 020333 (2022).
- [33] S. F. E. Oliviero, L. Leone, and A. Hamma, Magic-state resource theory for the ground state of the transverse-field Ising model, *Phys. Rev. A* **106**, 042426 (2022).
- [34] D. Rattacaso, L. Leone, S. F. E. Oliviero, and A. Hamma, Stabilizer entropy dynamics after a quantum quench, *Phys. Rev. A* **108**, 042407 (2023).
- [35] G. Passarelli, R. Fazio, and P. Lucignano, Nonstabilizerness of permutationally invariant systems, *Phys. Rev. A*

- 110, 022436 (2024).**
- [36] P. S. Tarabunga, Critical behaviors of non-stabilizerness in quantum spin chains, *Quantum* **8**, 1413 (2024).
  - [37] M. Bejan, C. McLauchlan, and B. Béri, Dynamical Magic Transitions in Monitored Clifford+T Circuits, *PRX Quantum* **5**, 030332 (2024).
  - [38] G. E. Fux, B. Béri, R. Fazio, and E. Tirrito, Disentangling unitary dynamics with classically simulable quantum circuits, [arXiv:2410.09001 \(2025\)](#).
  - [39] X. Turkeshi, A. Dymarsky, and P. Sierant, Pauli spectrum and nonstabilizerness of typical quantum many-body states, *Phys. Rev. B* **111**, 054301 (2025).
  - [40] G. Passarelli, P. Lucignano, D. Rossini, and A. Russomanno, Chaos and magic in the dissipative quantum kicked top, *Quantum* **9**, 1653 (2025).
  - [41] E. Tirrito, X. Turkeshi, and P. Sierant, Anticoncentration and nonstabilizerness spreading under ergodic quantum dynamics, [arXiv:2412.10229 \(2025\)](#).
  - [42] E. Tirrito, L. Lumia, A. Paviglianiti, G. Lami, A. Silva, X. Turkeshi, and M. Collura, Magic phase transitions in monitored gaussian fermions, [arXiv:2507.07179 \(2025\)](#).
  - [43] A. Russomanno, G. Passarelli, D. Rossini, and P. Lucignano, Nonstabilizerness in the unitary and monitored quantum dynamics of XXZ-staggered and Sachdev-Ye-Kitaev models, *Phys. Rev. B* **112**, 064312 (2025).
  - [44] J. Odavić, M. Viscardi, and A. Hamma, Stabilizer entropy in nonintegrable quantum evolutions, *Phys. Rev. B* **112**, 104301 (2025).
  - [45] M. Viscardi, M. Dalmonte, A. Hamma, and E. Tirrito, Interplay of entanglement structures and stabilizer entropy in spin models, [arXiv:2503.08620 \(2025\)](#).
  - [46] M. Collura, J. D. Nardis, V. Alba, and G. Lami, The non-stabilizerness of fermionic Gaussian states, [arXiv:2412.05367 \(2025\)](#).
  - [47] M. Sarkis and A. Tkatchenko, Are molecules magical? Non-Stabilizerness in molecular bonding, [arXiv:2504.06673 \(2025\)](#).
  - [48] G. C. Santra, A. Windey, S. Bandyopadhyay, A. Legramandi, and P. Hauke, Complexity transitions in chaotic quantum systems: Nonstabilizerness, entanglement, and fractal dimension in SYK and random matrix models, [arXiv:2505.09707 \(2025\)](#).
  - [49] T. Haug, L. Aolita, and M. Kim, Probing quantum complexity via universal saturation of stabilizer entropies, *Quantum* **9**, 1801 (2025).
  - [50] P. Sierant, P. Stornati, and X. Turkeshi, Fermionic magic resources of quantum many-body systems, [arXiv:2506.00116 \(2025\)](#).
  - [51] J. Huang, X. Qian, and M. Qin, Nonstabilizerness entanglement entropy: A measure of hardness in the classical simulation of quantum many-body systems with tensor network states, *Phys. Rev. A* **112**, 012425 (2025).
  - [52] L. G. Valiant, Quantum computers that can be simulated classically in polynomial time, in *Proceedings of the Thirty-Third Annual ACM Symposium on Theory of Computing, STOC '01* (Association for Computing Machinery, New York, NY, USA, 2001) p. 114–123.
  - [53] B. M. Terhal and D. P. DiVincenzo, Classical simulation of noninteracting-fermion quantum circuits, *Phys. Rev. A* **65**, 032325 (2002).
  - [54] T. Klein Kvarning, L. Herviou, and J. H. Bardarson, Time-evolution of local information: thermalization dynamics of local observables, *SciPost Phys.* **13**, 080 (2022).
  - [55] C. Artiago, T. Klein Kvarning, D. Aceituno Chávez, L. Herviou, and J. H. Bardarson, Universal characterization of quantum many-body states through local information, *Phys. Rev. Lett.* **134**, 190401 (2025).
  - [56] N. P. Bauer, B. Trauzettel, T. Klein Kvarning, J. H. Bardarson, and C. Artiago, Local information flow in quantum quench dynamics, *Phys. Rev. A* **112**, 022221 (2025).
  - [57] C. Artiago, J. Barata, and E. Rico, Out-of-equilibrium dynamics in a U(1) lattice gauge theory via local information flows: Scattering and string breaking, [arXiv:2510.16101 \(2025\)](#).
  - [58] C. Artiago, C. Fleckenstein, D. Aceituno Chávez, T. Klein Kvarning, and J. H. Bardarson, Efficient large-scale many-body quantum dynamics via local-information time evolution, *PRX Quantum* **5**, 020352 (2024).
  - [59] K. Harkins, C. Fleckenstein, N. D'Souza, P. M. Schindler, D. Marchiori, C. Artiago, Q. Reynard-Feytis, U. Basumallick, W. Beatrez, A. Pillai, M. Hagn, A. Nayak, S. Breuer, X. Lv, M. McAllister, P. Reshetikhin, E. Druga, M. Bukov, and A. Ajoy, Nanoscale engineering and dynamic stabilization of mesoscopic spin textures, *Sci. Adv.* **11**, eadn9021 (2025).
  - [60] P. S. Tarabunga, E. Tirrito, T. Chanda, and M. Dalmonte, Many-body magic via Pauli-Markov chains—from criticality to gauge theories, *PRX Quantum* **4**, 040317 (2023).
  - [61] D. Qian and J. Wang, Quantum nonlocal nonstabilizerness, *Phys. Rev. A* **111**, 052443 (2025).
  - [62] C. Cao, Non-trivial area operators require non-local magic, *JHEP* **11**, 105 (2024).
  - [63] C. Cao, G. Cheng, A. Hamma, L. Leone, W. Munizzi, and S. F. E. Oliviero, Gravitational back-reaction is magical, [arXiv:2403.07056 \(2025\)](#).
  - [64] P. S. Tarabunga and T. Haug, Efficient mutual magic and magic capacity with matrix product states, *SciPost Phys.* **19**, 085 (2025).
  - [65] H. Timsina, Y.-M. Ding, E. Tirrito, P. S. Tarabunga, B.-B. Mao, M. Collura, Z. Yan, and M. Dalmonte, Robustness of Magic in the quantum Ising chain via Quantum Monte Carlo tomography, [arXiv:2507.12902 \(2025\)](#).
  - [66] C. D. White, C. Cao, and B. Swingle, Conformal field theories are magical, *Phys. Rev. B* **103**, 075145 (2021).
  - [67] T. D. Ellison, K. Kato, Z.-W. Liu, and T. H. Hsieh, Symmetry-protected sign problem and magic in quantum phases of matter, *Quantum* **5**, 612 (2021).
  - [68] D. A. Korbany, M. J. Gullans, and L. Piroli, Long-range nonstabilizerness and phases of matter, *Phys. Rev. Lett.* **135**, 160404 (2025).
  - [69] D. Fattal, T. S. Cubitt, Y. Yamamoto, S. Bravyi, and I. L. Chuang, Entanglement in the stabilizer formalism, [arXiv:0406168 \(2004\)](#).
  - [70] V. Sharma and E. J. Mueller, Multipartite entanglement structures in quantum stabilizer states, *Phys. Rev. A* **112**, 012411 (2025).
  - [71] F. Y. Wu, The Potts model, *Rev. Mod. Phys.* **54**, 235 (1982).
  - [72] R. S. K. Mong, D. J. Clarke, J. Alicea, N. H. Lindner, and P. Fendley, Parafermionic conformal field theory on the lattice, *J. Phys. A* **47**, 452001 (2014).
  - [73] D. T. Smithey, M. Beck, M. G. Raymer, and A. Faridani, Measurement of the wigner distribution and the density matrix of a light mode using optical homodyne tomography: Application to squeezed states and the vacuum,

- [Phys. Rev. Lett. \*\*70\*\*, 1244 \(1993\)](#).
- [74] U. Leonhardt, Quantum-state tomography and discrete Wigner function, [Phys. Rev. Lett. \*\*74\*\*, 4101 \(1995\)](#).
  - [75] D. Leibfried, D. M. Meekhof, B. E. King, C. Monroe, W. M. Itano, and D. J. Wineland, Experimental determination of the motional quantum state of a trapped atom, [Phys. Rev. Lett. \*\*77\*\*, 4281 \(1996\)](#).
  - [76] A. I. Lvovsky and M. G. Raymer, Continuous-variable optical quantum-state tomography, [Rev. Mod. Phys. \*\*81\*\*, 299 \(2009\)](#).
  - [77] M. Cramer, M. B. Plenio, S. T. Flammia, R. Somma, D. Gross, S. D. Bartlett, O. Landon-Cardinal, D. Poulin, and Y.-K. Liu, Efficient quantum state tomography, [Nat. Commun. \*\*1\*\*, 149 \(2010\)](#).
  - [78] I. M. Flór, C. Artiago, T. Klein Kvorning, and J. H. Bardarson, The higher-dimensional information lattice, In preparation (2025).
  - [79] S. Sang, Y. Zou, and T. H. Hsieh, Mixed-state quantum phases: Renormalization and quantum error correction, [Phys. Rev. X \*\*14\*\*, 031044 \(2024\)](#).
  - [80] S. Sang, L. A. Lessa, R. S. K. Mong, T. Grover, C. Wang, and T. H. Hsieh, Mixed-state phases from local reversibility, [arXiv:2507.02292 \(2025\)](#).